Development of a High Pulse Rate EUV Source

Stephen F. Horne, Fred M. Niell, Matthew J. Partlow, Matthew M. Besen,
Donald K. Smith , Paul A. Blackborow, Deborah Gustafson
Energetiq Technology, Inc

ABSTRACT

The Energetiq EQ-10 is a medium-power (10 W/2π, 13.5nm +/- 1%, Xenon) EUV source suitable for a variety of mirror testing, resist exposure, and defect inspection applications. The EQ-10 was designed to operate at a pulse frequency of 1 to 2 kHz[1]. However, exposure equipment appropriate for High Volume Manufacturing (HVM) requires sources which are projected to operate at 10 kHz or greater[2]. To minimize technical risk in infrastructure development programs now under way in support of future HVM production, scaling of various physical processes with pulse rate require investigation. A program to redesign the EQ-10 to operate at 10 kHz pulse rate has been completed. We report here on the design process and the operating characteristics of the high-frequency source.

Keywords: Z-pinch, electrodeless, EUV

1. INTRODUCTION

Development of support infrastructure for HVM relies on reasonable extrapolation from data derived using technology available currently and in the near term; however conservative engineering practice requires that the inherent technical risk be minimized. There is specific concern, for instance, that optics degradation/contamination may have a dependence on pulse frequency as well as (or instead of) integrated dose. We have developed an electrodeless Z-pinch based source operating at 10 kHz, based on the successful EQ-10 design. In this paper we will describe the operation of the source in sufficient detail to illuminate some of the issues involved, and give measured performance data for the upgraded source.

2. THEORY OF OPERATION

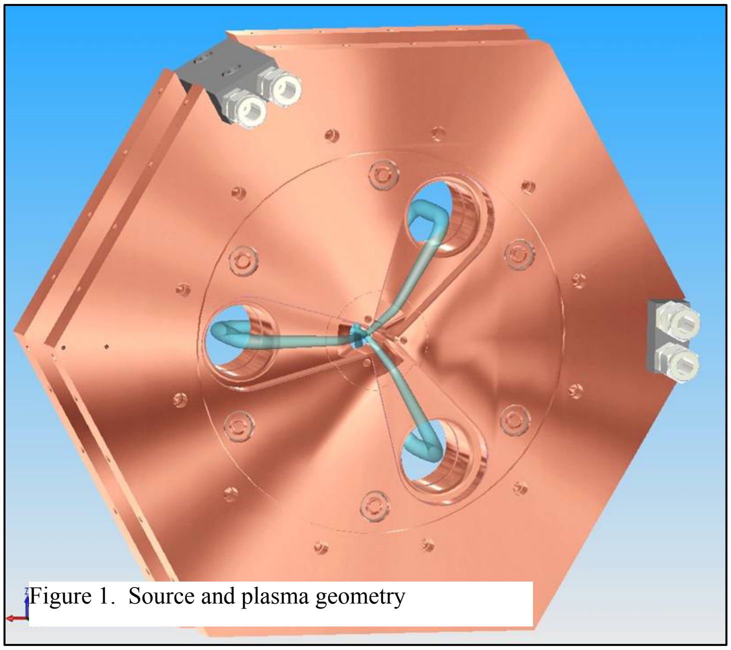

Figure 1. Source and plasma geometry

The EQ-10[1] is a discharge plasma Z-pinch source which relies on induction via a transformer core, rather than conduction via electrodes, to generate the Z-pinch current. In the basic design, the transformer primary circuit consists of two copper plates, connected by a conductive tube at the center. The primary current flows radially in on one plate, axially through the central connection, and radially outward through the second plate. The induced secondary currents flow in a plasma through three electrically parallel paths which pierce the primary structure in three places (the plasma return holes), and then combine in the central bore. Figure 1 shows this geometry.

Sandwiched between the plates are two magnetic cores. The inner core, closely surrounding the central bore, provides the magnetic flux linkage between the primary current path through the copper, and the three parallel secondary currents flowing in the plasma, which combine in the bore to generate the magnetic Z-pinch. The second core is near the outer radius of the device, and surrounds the three plasma return holes. This core functions as a magnetic switch with a specific volt-second capacity. Figure 2 shows a cross-section of the structure.

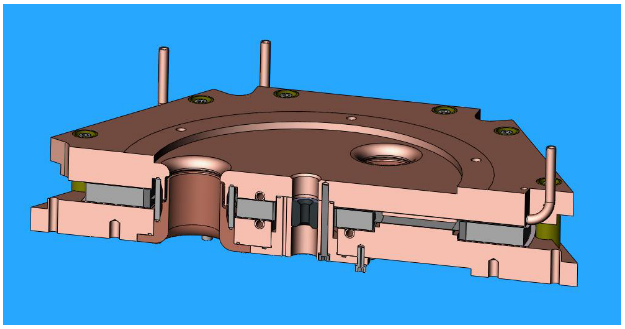

Figure 2. Cross-section details.

In operation, a capacitor bank (not shown) is connected across the copper plates – symmetrically, with connections to each of the six facets of the copper plates. A fast electrical pulse (derived from a pulse forming system – not shown) is applied to the plates, causing the capacitors to begin to charge. In parallel, a current flows through the copper structure – in one plate, through the bore, out the other plate. The magnetic switch acts as a high impedance (effectively, a series inductance) during this charging process, allowing only a small leakage current to flow – until the switch core saturates. At this point the core becomes essentially zero inductance, allowing the now charged capacitor bank to appear across the inner induction core. The current and magnetic field in the core ramps, generating an EMF which drives current in the plasma through the bore and plasma return holes. The plasma current flowing through the bore of the device generates its own local magnetic field, which acts to compress the plasma current channel. When this field becomes intense enough, a dynamic pinch occurs, which collapses the current channel to less than 1 mm diameter in a few tens of nanoseconds – thus compressing and heating the plasma to the point where EUV emission occurs. Figure 3 shows a simplified schematic.

The geometric design of the system deserves mention. The objective, of course, is to ramp the plasma current as quickly as possible. This current is linked to the primary current by the mutual inductance of the inner core. All other sources of stray inductance must be minimized. On the primary side of the circuit, the symmetric parallel plate design accomplishes this goal. On the plasma side, spreading the current among three paths significantly reduces the plasma self-inductance; the large diameter of the return holes (compared to the bore) further reduces the inductance.

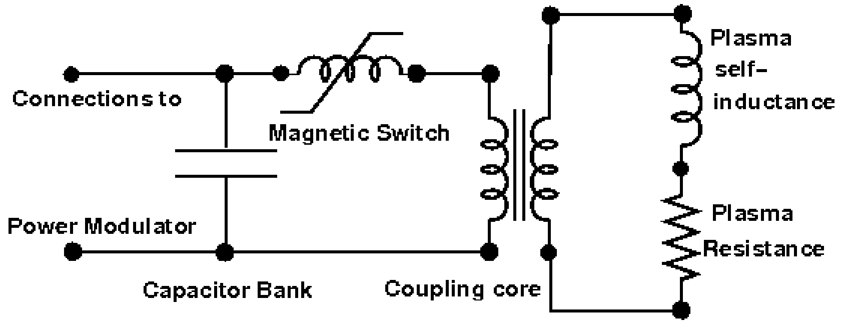

Figure 3. Simplified schematic diagram

A complication (from the electrical engineer's point of view) is that the resistance of the plasma loop is not negligible and further is a complex function of both electrical parameters (such as primary voltage and frequency) and physical parameters (such as gas pressure and composition). Thus, once the purely electrical and thermal problems have been addressed, the determination of an optimal operating point remains. The source operating point is a compromise among many factors, including pulse energy, pulse rate, thermal effects in the magnetics and bore, neutral gas density in the chamber, and degree of preionization of the plasma. Operation at high frequency either requires or causes changes in all these factors. Increasing pulse rate while holding total power consumption roughly constant, entails reducing pulse energy. Frequency-dependent losses in magnetic materials force a significant electrical and thermal redesign of the pulse forming electronics. The increased pulse rate raises both the plasma and the neutral gas temperature, affecting both the trajectory of the plasma current pulse, and the boundary conditions for the Z-pinch – requiring a re-optimization of the operating point to achieve EUV emission conditions.

3. DESIGN PROCESS AND MODELING

In the standard EQ-10, the operating cycle – capacitor charging, core switching, capacitor discharging, plasma current ramp, and pinch formation – occurs at between 1 and 2 KHz, depending on the chosen operating point. At the nominal operation frequency of 1800 Hz, the device produces 10-12 W inband, with about 4000 -5000 W of DC power supplied to the power modulator. The goal of the high frequency design was to hold input DC power roughly constant, while increasing the source operating frequency to 10 KHz. No attempt was made to hold output EUV power constant; it was recognized that many of the parasitic losses in the system would scale as frequency, and wall plug efficiency would be reduced as a result. An engineering goal of 2 W of inband power was defined, however. This goal implies 0.2 mJ per pulse of in-band EUV to be produced in the high-frequency system – compared to about 6 mJ/pulse in the standard EQ10, for a reduction in per-pulse output by a factor of order 30.

The design effort was guided by a model developed as a full nonlinear treatment of the pulse forming system (or modulator), the source itself from an electrical point of view, and the plasma pinch process, to the extent that it presents a dynamic load to the electrical system. **Figure 4** shows the system as modeled. As can be seen, there are two stages of pulse compression in the final design. The model was developed as a Matlab application, which allowed a full, detailed nonlinear treatment of the magnetic switch cores. These are the most critical components of the design – surprisingly, more critical than the plasma itself – from the electrical point of view.

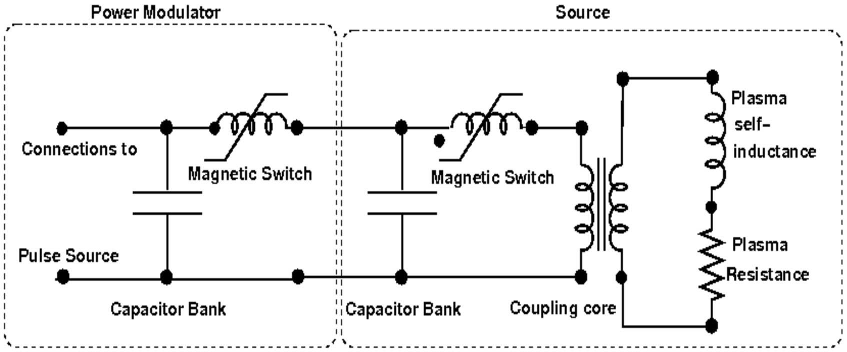

Figure 4. Modeled electrical system.

While the system does not appear particularly complex at first glance, one should appreciate that what we have here is a coupled pair of driven, damped, nonlinear oscillators – with a nonlinear load. Mechanical analogues of similar (and much simpler!) design are often studied as exemplars of chaotic orbital dynamics. Software circuit simulators such as SPICE cannot easily manage multiple coupled non-linear magnetic elements in time-domain analysis[3], and introducing the plasma load would introduce further complexities. Ultimately, it is a less complex path to begin with Maxwell's equations and propagate them forward with a standard solver. The complexities end up being in the geometry and boundary conditions of the system. The unique geometry of the EQ10 ultimately informs and simplifies much of the initial work in setting up the equations; geometric symmetry eases the modeling of inductances and capacitances. The general approach involved a Kirchov's law description of the system in differential form while adding a few more coupled differential equations to handle the plasma snowplow model[4], with the non-linear terms handled in a piece-wise time-domain fashion. In all, 12 simultaneous non-linear differential equations are required to replicate the EQ10 operation faithfully.

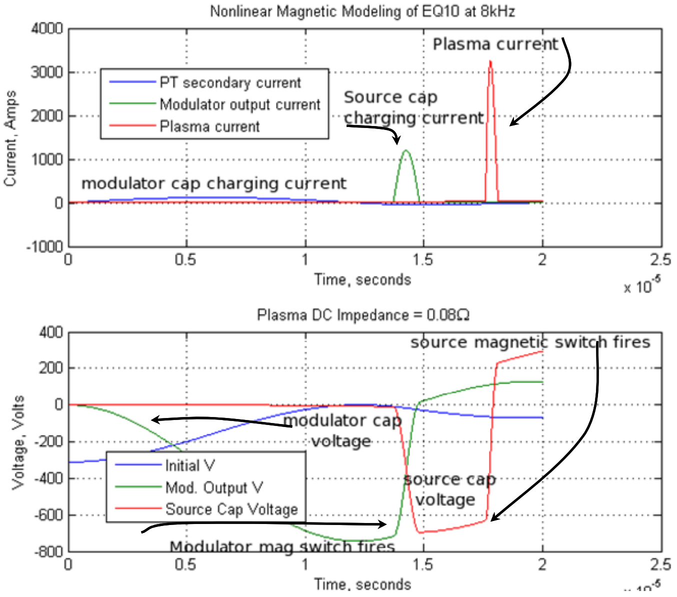

Figure 5. Modeled source electrical parameters

The model evolved in the following way. First, the magnetic switch parameters were defined. Since power dissipation per unit volume in the magnetic core material scales linearly with frequency, and the frequency was to increase by a factor of five, the volume of core material cannot be held constant.

By reducing the core height and (therefore volume) by a factor of two relative to the EQ10, the cooling was improved by a factor of four, while reducing the heat per pulse dissipated by the core by a factor of two. Of course, the volt-seconds required to switch the core is reduced as well. The volt-second reduction then drives the capacitance down by the same factor, assuming no change in pulse rise times. These decisions define most of the parameters of the model.

Once the basic model was functional, it was used to estimate the safe operating region (both electrically and thermally) of the system.

Figure 5 shows typical model output. The upper panel displays currents, the lower voltages. At t=0, a current pulse begins to charge the modulator capacitor bank. The capacitor voltage ramps negatively and at about 14 microseconds into the pulse, the modulator magnetic switch saturates, switching from a high-inductance to a very low inductance state. The modulator bank discharges over a period of about 10 microseconds, transferring charge to the source capacitor bank. The source bank holds its voltage for about 400 microseconds, until the source magnetic switch saturates. The bank then discharges over a period of a few microseconds. The coupling core effectively distributes the source bank voltage around the plasma path as an electric field, which causes about 3000 amperes of current to flow in the plasma loops.

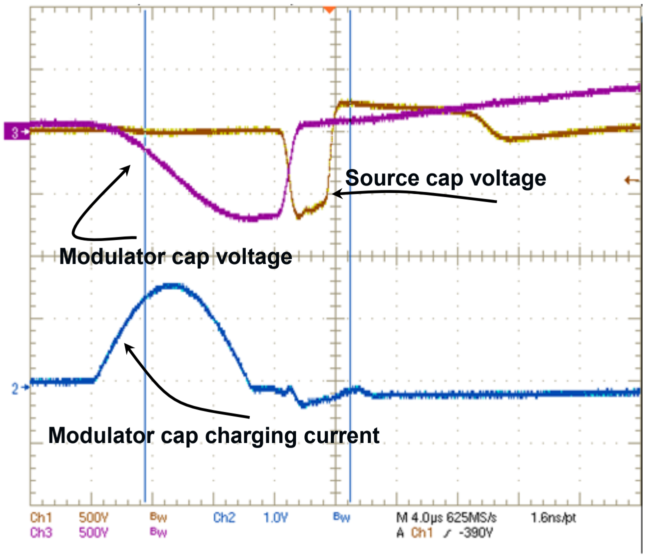

Figure 6. Measured source electrical parameters

Error! Reference source not found. Figure 6 shows measured currents and voltages to compare to **Error! Reference source not found.**Figure 5, for conditions similar to those modeled. The timescale is 4 microseconds per box; voltage scales (top two traces) are 500 V/box. Good agreement is seen both in amplitude of the various signals, and in the time evolution of the system.

4. RESULTS AND ANALYSIS.

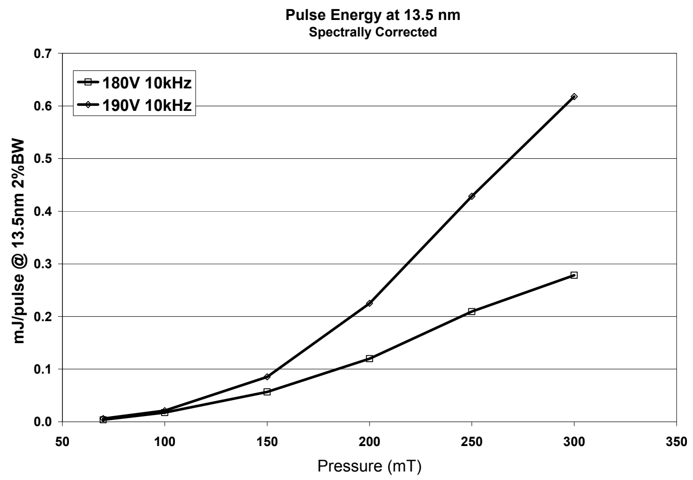

Figure 7. In-band joules/pulse

The in-band EUV power was measured using a diagnostic based on a narrow-band multilayer mirror and a silicon diode. The diagnostic calibration is NIST-traceable. Data were measured at two different DC input voltages, and over a range of source pressures; the results are shown in **Figure 7**. Two effects are obvious. First, a small change in DC input to the system results in about a factor of two change in output power. This effect is due to the fact that the EUV output is a very non-linear function of the pinched plasma parameters. The device operates in Xenon; the primary source of EUV radiation derives from the Xe +10 ion, which requires 229 eV of energy to create. The electron temperature of the pinched plasma is in the 40 ev range; hence the electrons with sufficient energy to create the necessary ions are far out on the tail of the distribution – and their number is very sensitive to small changes in plasma temperature.

The second effect – that the EUV output increases with pressure – is, we believe, due to pinch fueling. In the EQ10, running at 1800 Hz, a maximum in output is seen, typically at 100 mT or less. Output decreases above that pressure. In contrast, at 10 kHz, we see a monotonic increase in output up to 300 mT – the maximum pressure tested. We presume that the neutral gas temperature in the region of the pinch is significantly higher in the 10 kHz case, leading to an equivalently reduced xenon density there. Therefore, higher pressure is required to provide adequate density to fuel the pinch. Finally, it should be noted that the design goal for the system – 0.2 mJ per pulse, inband – was achieved.

Figure 8 shows the broadband power available from the source, shown in terms of Joules per pulse. This is a line-of-sight measurement through a zirconium foil, which yields a bandpass roughly from 5 to 15 nm. The shapes of the pulse energy curves versus pressure are similar to the inband measurements, but the values are higher by a factor of order 25-30. While imaging applications usually require narrow bandwidth to avoid chromatic effects, and the multi-layer mirror technology used in mirrors and masks rely on narrow bandwidth, many infrastructure development applications do not. Grazing incidence optics can provide excellent focusing characteristics over a broad wavelength band, allowing a high quality focus to be achieved. Thus a very high EUV flux can be made available for applications such as mirror testing and resist development, where narrow-band radiation is not an absolute requirement.

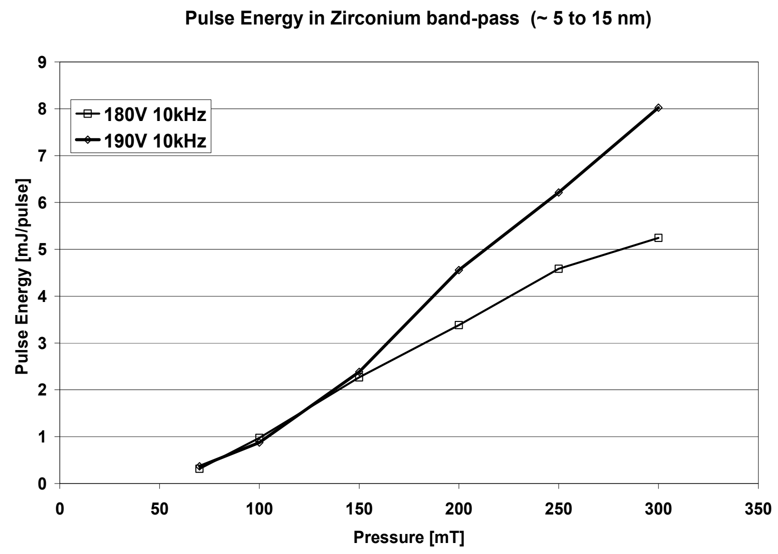

Figure 8. Broad-band joules per pulse

Geometric stability of the source can be an issue primarily for imaging systems. We have developed a mechanically robust imaging system that enables very repeatable measurement of plasma size and position. **Figure 9**shows the plasma size (FWHM) measured over a 75 minute interval. Over this period, the plasma size varied by about +/- 10 microns, around an average value of 530 microns.

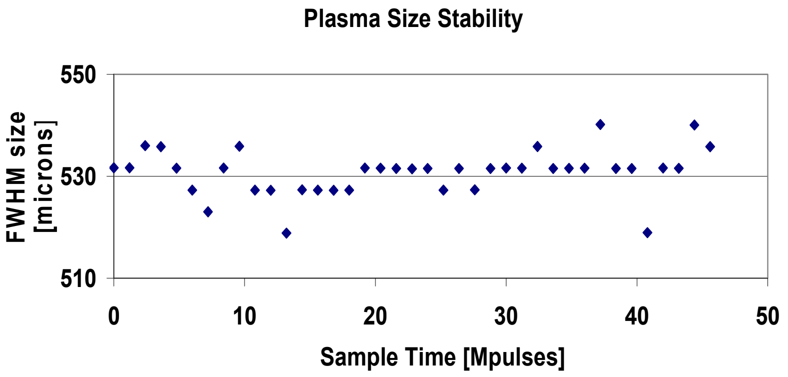

Figure 9. Plasma size stability

Plasma positional stability in this type of source is excellent by any measure. Because the pinch discharge is not initiated on electrodes, there is no geometric jitter due to variation in breakdown position. The pinch evolves subject only to magnetic forces, which ultimately are carried by massive, precision machined conductive structures**.** Figure 10 represents our latest attempt to measure the position variation of the pinch. We see less than 10 micron variation vertically, and essentially zero horizontally. There is no reason to believe that the plasma knows "which way is up" and it is quite possible that the vertical variation is due to a mechanical drift of the camera support structure, in response to temperature variation. For reference, we display a 30 micron radius circle.

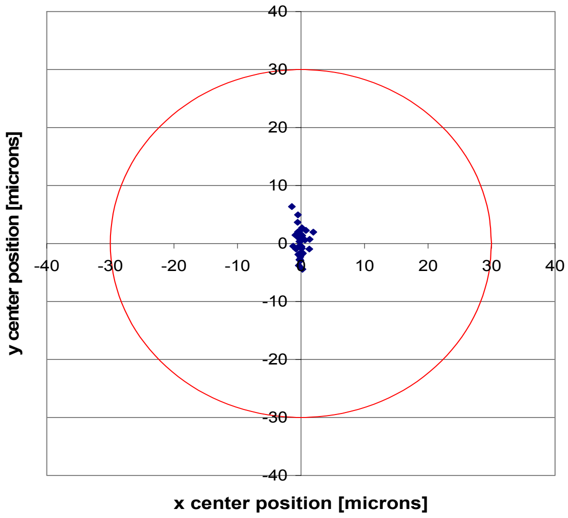

Figure 10. Plasma positional stability

CONCLUSIONS

We have developed and made commercially available an electrode-less discharge plasma Z-pinch source of 13.5 nm EUV radiation, operating at 10 kHz. The design was guided by the successful EQ-10 device, and scaled both in frequency and EUV pulse amplitude to hold input wall-plug power roughly constant. Nonlinear numerical modeling of the device played a large role in the design process. Detailed characterization of the assembled source revealed no significant issues and all design goals were achieved. The device is suitable for applications in EUV infrastructure development, wherever high pulse rates are required.

REFERENCES

[1] Blackborow, P.A., Partlow, M.J., Horne, S.F., Besen, M.M., Smith, D.K., D. S. Gustafson, D.S., "EUV Source Development at Energetiq," Emerging Lithographic Technologies XII 6921(1), p. 692121, SPIE, (2008).

[2] Brandt, D.C. et al, "LPP EUV source development for HVM," Emerging Lithographic Technologies XI 6517, p. 65170, SPIE, (2007).

[3] Smith, P. W. [Transient Electronics: Pulsed Circuit Technology], Wiley, Chichester, (2002)

[4] Seshadri, S. R., [Fundamentals of Plasma Physics] , American Elsivier Publishing Co. Inc., New York, (1973)